Laboratory performance of the shaped pupil coronagraphic architecture for the WFIRST-AFTA coronagraph

Eric Cady[a*], Camilo Mejia Prada[a], Xin An[a], Kunjithapatham Balasubramanian[a], Rosemary Diaz[a], N. Jeremy Kasdin[b], Brian Kern[a], Andreas Kuhnert[a], Bijan Nemati[a], Keith Patterson[a], Ilya Poberezhskiy[a], A. J. Eldorado Riggs[b], Daniel Ryan[a], Hanying Zhou[a], Robert Zimmer[a], Neil T. Zimmerman[b]

[a] Jet Propulsion Laboratory, California Institute of Technology, Pasadena, CA, 91109 USA
[b] Department of Mechanical and Aerospace Engineering, Princeton University, Princeton, NJ, 08540 USA

ABSTRACT

One of the two primary architectures being tested for the WFIRST-AFTA coronagraph instrument is the shaped pupil coronagraph, which uses a binary aperture in a pupil plane to create localized regions of high contrast in a subsequent focal plane. The aperture shapes are determined by optimization, and can be designed to work in the presence of secondary obscurations and spiders—an important consideration for coronagraphy with WFIRST-AFTA. We present the current performance of the shaped pupil testbed, including the results of AFTA Milestone 2, in which $\approx 6 \times 10^{-9}$ contrast was achieved in three independent runs starting from a neutral setting.

1. INTRODUCTION

WFIRST-AFTA (WFIRST: Wide Field InfraRed Survey Telescope, AFTA: Astrophysics-Focused Telescope Assets) [1] is a proposed 2.4m telescope with a wide-field infrared array to investigate dark energy, as well as track microlensing events and perform wide-field survey science. The WFIRST-AFTA coronagraph is a second instrument for the observatory, designed to capture the reflected light from large terrestrial and gas giant planets around nearby stars while suppressing that of the nearby star.

The original pupil of the WFIRST-AFTA telescope had a large obscuration, spiders, and other small features, as seen in Figure 1. As most extant high-performing coronagraphs were designed for unobscured apertures, new designs were required that were compatible with this pupil while still providing high performance. The instrument contains two coronagraphic architectures optimized to the WFIRST-AFTA pupil, a shaped pupil coronagraph (SPC) [2, 3] and a hybrid Lyot coronagraph (HLC) [4], which may be interchanged or removed entirely with filter wheels. The combined coronagraph has been termed the Occulting Mask Coronagraph (OMC). A phase-induced amplitude-apodization complex-mask coronagraph (PIAACMC) [5] serves as a backup option.

Each of the coronagraphs selected for the WFIRST-AFTA coronagraph required new technology to be compatible with the pupil. For the SPC, it was the use of a reflective pupil mask, instead of a transmissive one; for the HLC, it was the development of a circular focal plane mask, instead of a linear one. A series of 9 milestones were laid out to provide a concrete roadmap for technology demonstration over a three-year period. In this paper, we discuss two of these milestones involving contrast demonstrations for the shaped pupil coronagraph:

- Milestone 2: The shaped pupil coronagraph in the High Contrast Imaging Testbed demonstrates 10^{-8} raw contrast with narrowband light at 550 nm in a static environment.
- Milestone 5: The Occulting Mask Coronagraph in the High Contrast Imaging Testbed demonstrates 10^{-8} raw contrast with 10% broadband light centered at 550 nm in a static environment.

* eric.j.cady@jpl.nasa.gov
©2015 California Institute of Technology. Government sponsorship acknowledged.

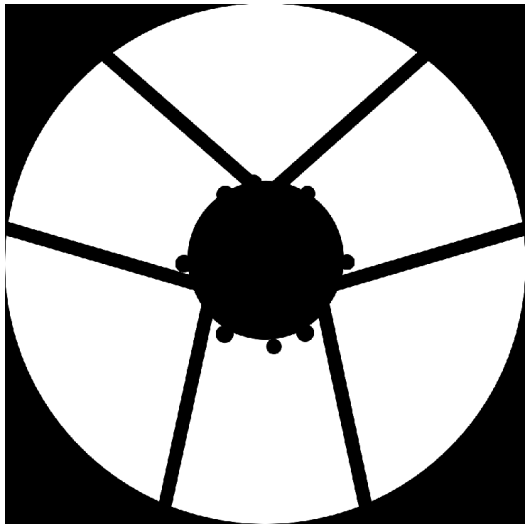

Figure 1. The AFTA pupil presented to the coronagraph design teams in 2013.

Here we use "raw" contrast to indicate that these levels must be achieved without postprocessing to subtract off the residual point spread function. Milestone 2 was due on September 30th, 2014, and for it we demonstrated 6×10^{-9} contrast in a 2% band centered at 550nm. Milestone 5 is scheduled to be completed in September of 2015.

Section 2 will give a further overview of the coronagraph design and hardware, while sections 3 will present the results and status of Milestones 2 and 5.

2. DESIGN AND HARDWARE OVERVIEW

The concept of a shaped pupil coronagraph is based on Fourier optics, and the Fourier-transform relationship between fields in a pupil and a focal plane. If we start with a circular pupil (or one that looks like Figure 1, in the WFIRST-AFTA case), and block open regions of the pupil, we can change the distribution of the light in the focal plane. With appropriate amplitude optimization of the area blocked [2, 3], we can shape the pupil such that the point spread function (PSF) in the focal plane has areas where the residual light is highly suppressed; Figure 2 shows a pupil optimized for the WFIRST-AFTA telescope, and resulting PSF. A field stop may then be added to block the light outside the "dark hole"—the coronagraph region of interest—preventing the detector from saturating. The dark holes are generally pairs of annular wedges, and the field stops are often called "bowtie masks" for this shape. As with all other coronagraphs, aberrations on optics and misalignments between optics diffract unwanted light into the dark hole, and deformable mirrors (DMs) are used to correct those errors.

Milestone 5 uses a variant of the shaped pupil coronagraph called a shaped pupil Lyot coronagraph (SPLC)[3, 6], which puts a Lyot stop in an intermediate pupil between the bowtie mask and the focal plane at the camera. With a Lyot stop present, the bowtie mask is no longer simply a field stop, but an active part of the diffraction control which requires tighter alignment tolerances. In exchange for this, the coronagraph as a whole achieves a smaller inner working angle and a higher contrast, enabling increased science yield. SPLC masks for Milestone 5 are shown in Figure 3.

The designs for the SPC and SPLC pupils both have isolated regions, which makes them difficult to manufacture as freestanding transmissive optics, as previous shaped pupils have been [7, 8]. Instead, a reflective shaped pupil was developed [9], using an aluminum coating on a thick silicon wafer as the reflective surface and black silicon processing [10] to absorb incident light in the blocked regions. Figure 4 shows microscope images of the manufactured pupils. On the other hand, the bowties and Lyot stops can be freestanding, and the holes in each were made by deep reactive ion etching of thin silicon wafers [7]. Images of an array of bowties and a mounted Lyot stop are shown in Figure 5 and Figure 6, respectively.

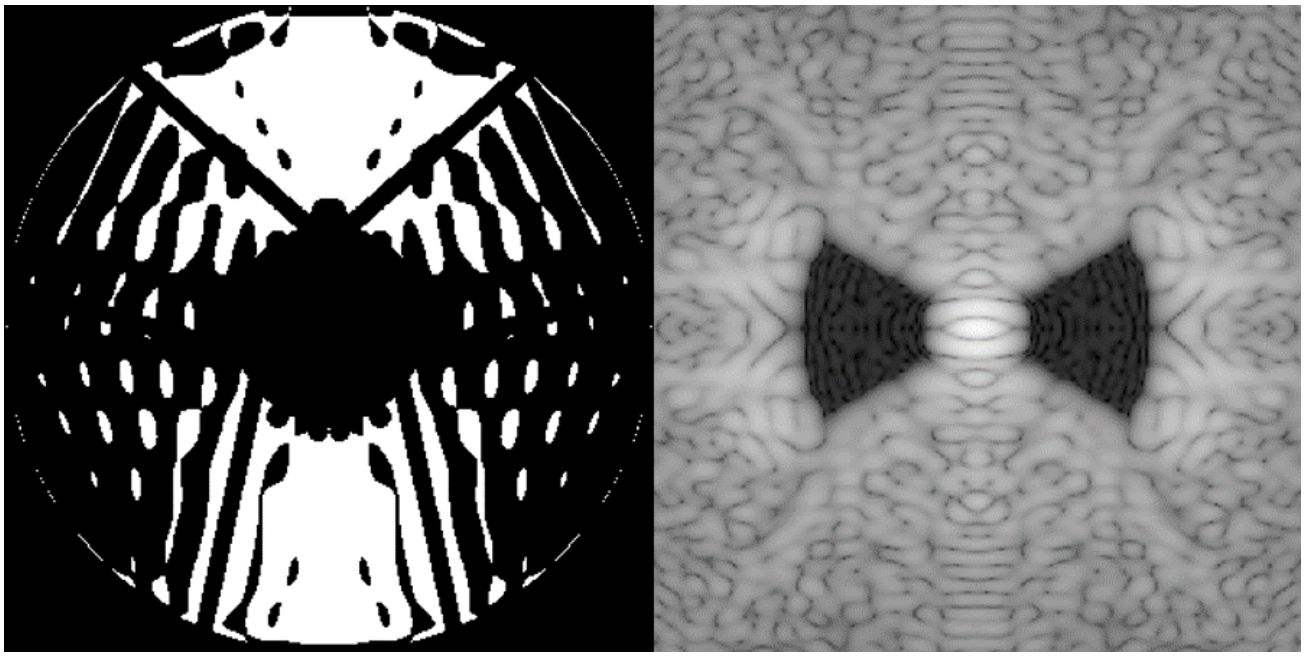

Figure 2. *Left.* A shaped pupil coronagraph pupil mask. *Right.* Point spread function for this pupil.

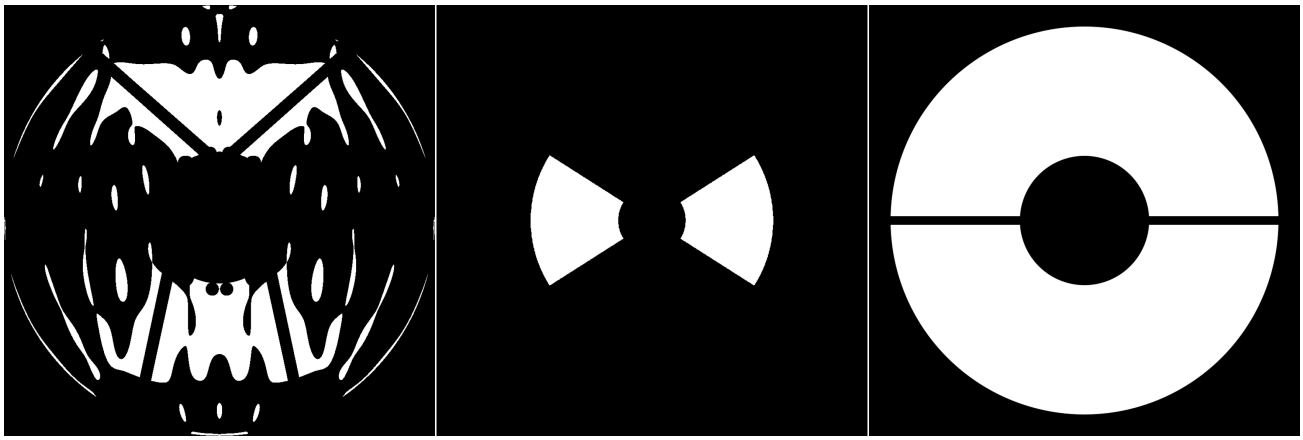

Figure 3. Shaped pupil Lyot coronagraph masks: *Left.* Shaped pupil. *Center.* Bowtie focal plane mask. *Right.* Lyot stop.

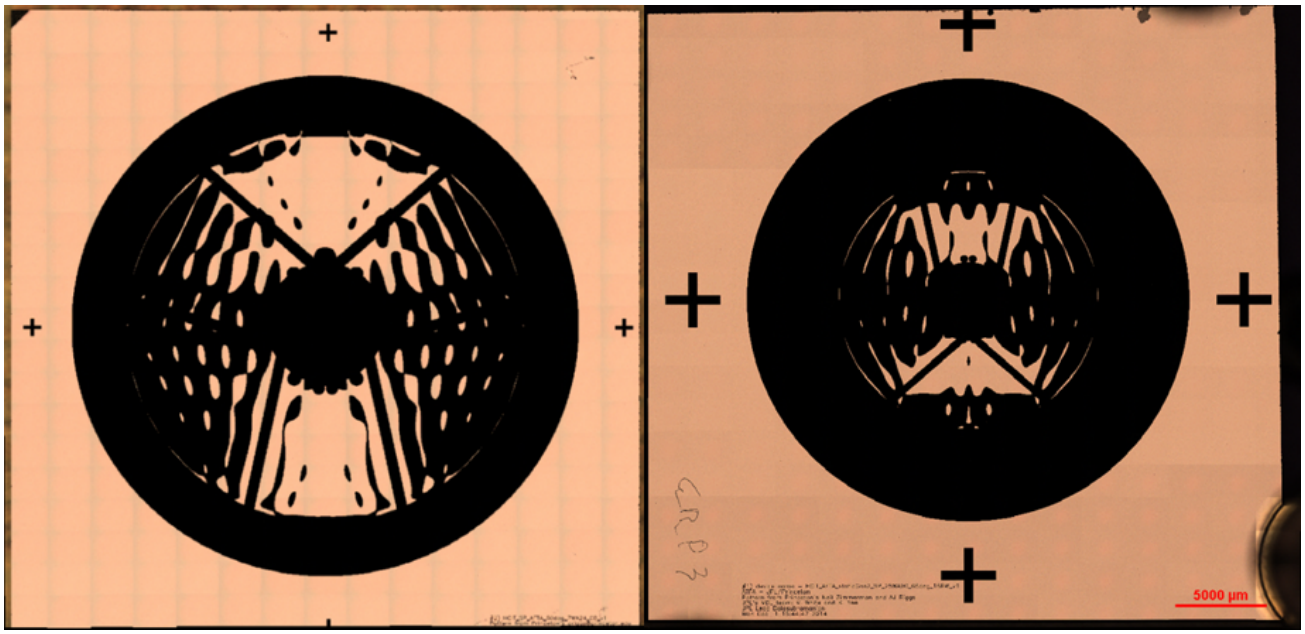

Figure 4. *Left.* A high-resolution microscope image of the Milestone 2 mask. *Right.* A high-resolution microscope image of the Milestone 5 mask.

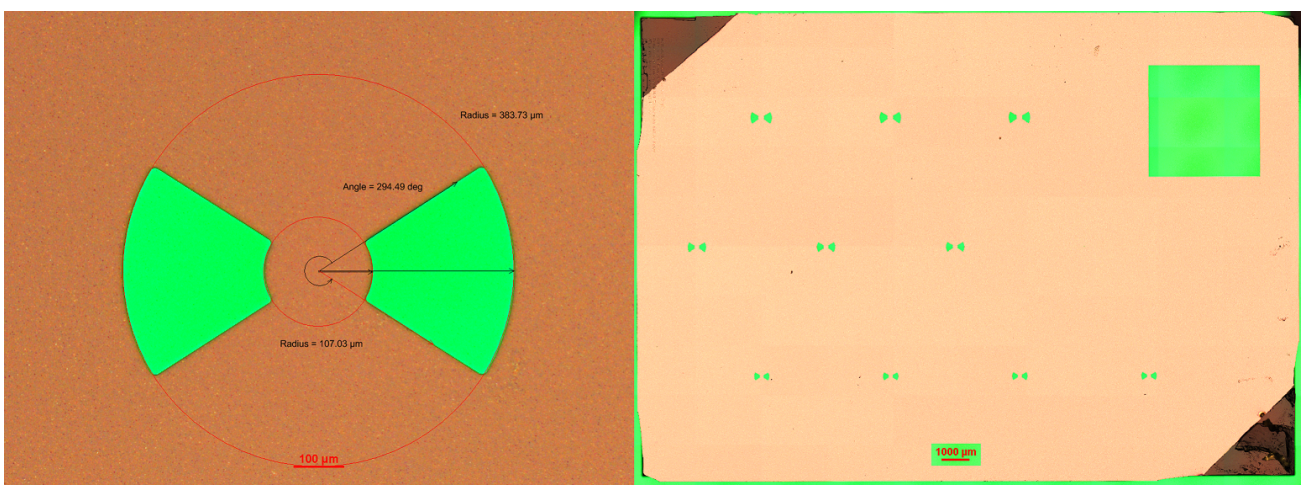

Figure 5. *Left.* A high-resolution microscope image, in transmission, of a single SPLC bowtie mask. *Right.* A high-resolution microscope image, in transmission, of an array of SPLC bowtie masks. All are $2.5 - 9\lambda/D$, but designed for different wavelengths.

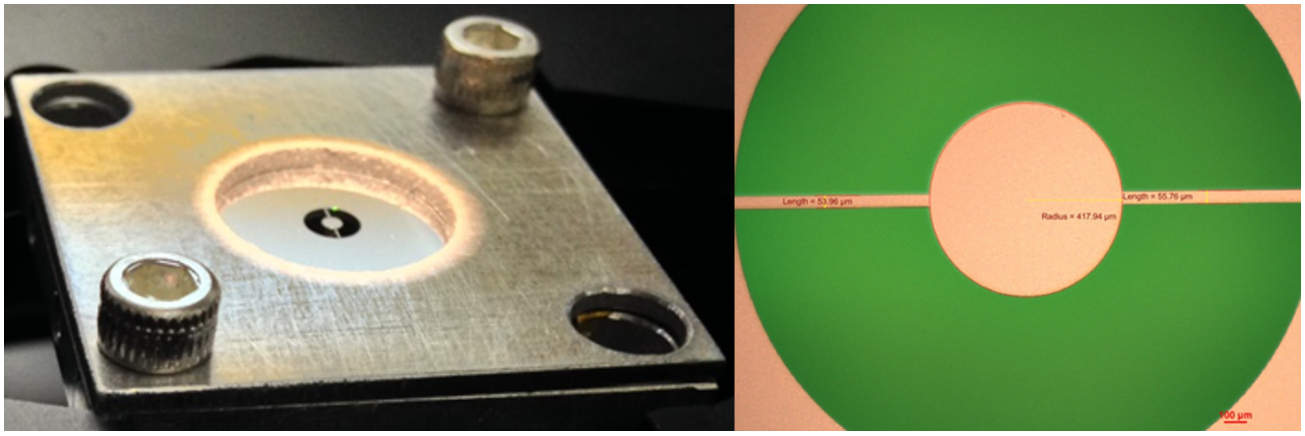

Figure 6. *Left.* An SPLC Lyot mask mounted in its holder in preparation for microscopy. *Right.* A high-resolution microscope image, in transmission and reflection, of the same Lyot stop.

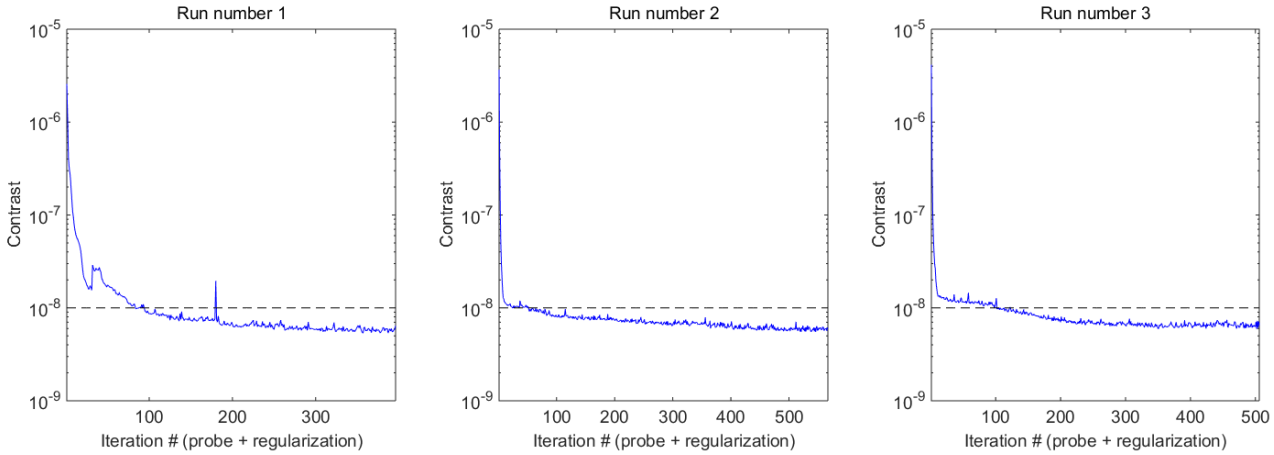

Figure 7. Mean contrast across the dark hole as a function of iteration number, for each of the three Milestone 2 runs.

3. MILESTONE 2 AND 5 RESULTS

Milestone 2 was intended to demonstrate high contrast with a baseline shaped pupil coronagraph, using a single DM to create a dark hole on one side of the image plane. The reasons for this were logistical—we had a single 64x64-actuator Xinetics DM ready to use with the testbed at the time of assembly, and expected to insert a second DM later when it became available. The shaped pupil in Figure 2 was installed, along with a bowtie with a dark hole from $4.4 - 11.2\lambda_0/\mathrm{D}$, with a central wavelength $\lambda_0 = 550$nm and a diameter set by the extent of the shaped pupil.

The data for Milestone 2 consisted of three separate wavefront correction trials in a 2% band centered at 550nm, starting from a flat DM setting each time. Each time the testbed was allowed to run until the contrast ceased to converge; the iteration sequences are shown in Figure 7. Mean contrast over the final 100 iterations was $(5.85 \pm 0.49) \times 10^{-9}$, $(5.95 \pm 0.49) \times 10^{-9}$, and $(6.59 \pm 0.56) \times 10^{-9}$, respectively over the three runs. A typical high-contrast image is shown at top left in Figure 8, along with a image of the testbed with the same DM setting, but using a 10%-band filter. Azimuthal averages are given at the bottom. (For a more detailed description of the testing and analysis, see 11.)

The SPLC was created and designed while Milestone 2 was ongoing, and eventually was selected to succeed the baseline SPC. Accordingly Milestone 5 was performed using a new SPLC rather than the coronagraph from Milestone 2. The bowtie is open $2.5 - 9\lambda_0/\mathrm{D}$ over symmetric 65° wedges, again with a central wavelength $\lambda_0 = 550$nm and the shaped pupil setting the pupil diameter. However, with the Lyot stop present, the inner

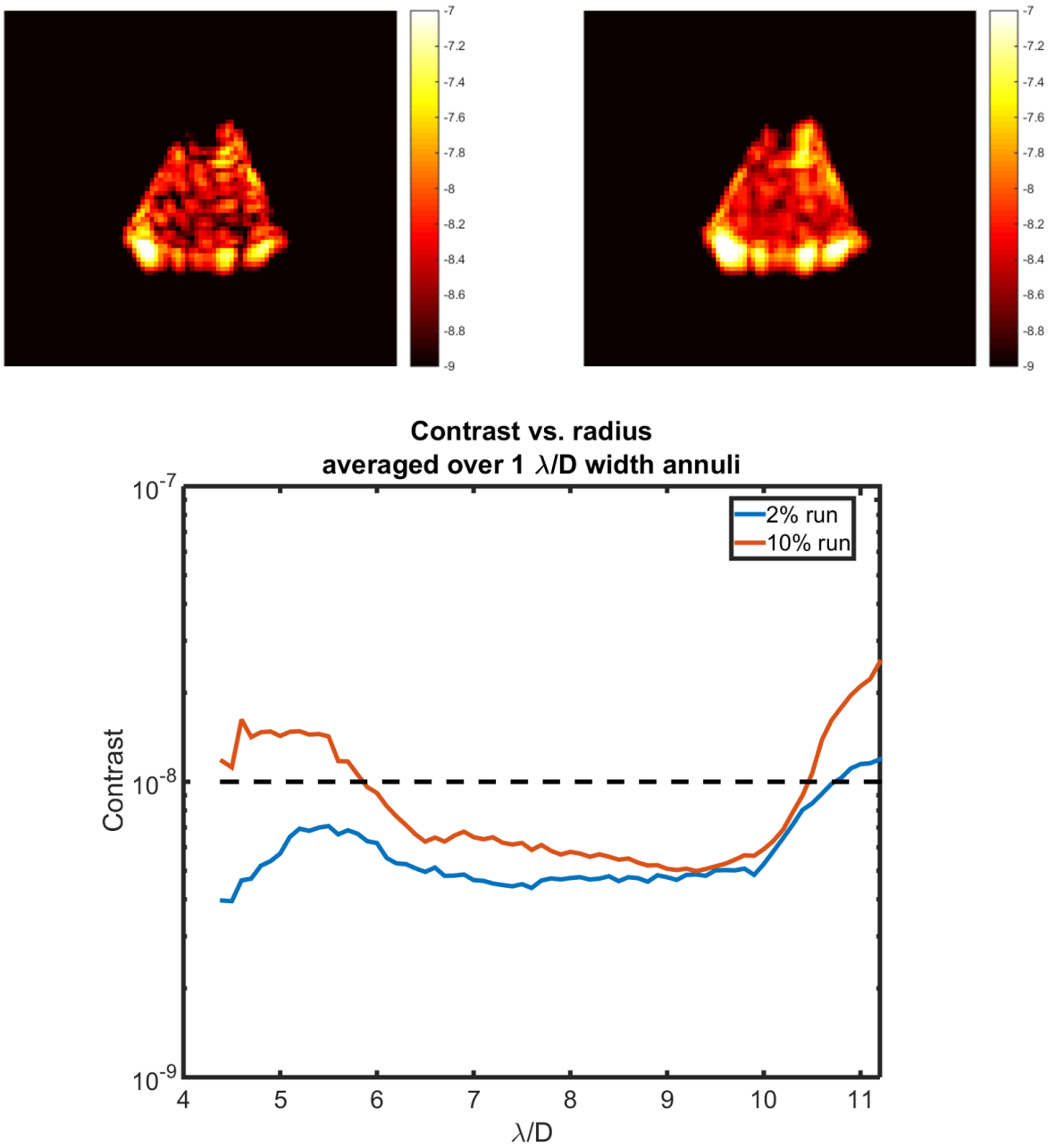

Figure 8. *Top left:* Dark hole in 2% band centered at 550nm. *Top right:* Dark hole in 10% band centered at 550nm, taken with same DM setting. Results are in units of contrast, on a $\log_{10}$ scale. *Bottom:* Azimuthally-averaged contrasts for the left and right images.

working angle is $\approx 2.8\lambda/D$. The Lyot stop is annular, with the outer diameter undersized by 10% and a 30% central obstruction.

Upgrading from the Milestone 2 configuration to one usable for the shaped pupil Lyot coronagraph required several modifications to the testbed:

- A second deformable mirror was introduced 1m downstream from the first, to permit the simultaneous correction of amplitude and phase on both sides of the PSF.
- The shaped pupil mask and array of bowtie masks were replaced, and a Lyot stop was added downstream of the bowtie array, along with a 3-axis stage for fine alignment. The testbed model was also updated accordingly.
- The control scheme was changed from using a single 2% band for control, in favor of collections of 2% bands spanning and bounding a 10% overall band.

While data collection for the milestone is still ongoing, early results are promising. As of the start of August 2015, the best contrast achieved was 1.39×10^{-8}, averaged over 5 2% subbands spanning a 10% band running from $522.5 - 577.5$nm. Fig. 9 shows both the individual bands and the contrast for a 10% band, assuming a flat spectrum. We expect to have the contrast better than 1×10^{-8} by the Milestone date of September 15, 2015, which would satisfy the Milestone requirement.

4. FUTURE DIRECTIONS

Following the completion of Milestone 5, our efforts will be directed towards upcoming milestones, particularly Milestone 9. Milestone 9 requires demonstration of 10^{-8} contrast with OMC in a 10% band, but in a simulated dynamic environment, with a telescope simulator introducing realistic and calibrated errors into the system and a low-order wavefront sensor and controller attempting to remove them while maintaining contrast. A separate bench is being assembled to co-mount an SPLC and an HLC. This milestone is scheduled to be completed by the end of September 2016, and will be the final technology development milestone for the WFIRST-AFTA coronagraph prior to reaching Technology Readiness Level 5.

ACKNOWLEDGMENTS

This work was performed at the Jet Propulsion Laboratory, California Institute of Technology, under a contract with the National Aeronautics and Space Administration.

References

[1] D. Spergel, N. Gehrels, C. Baltay, D. Bennett, J. Breckinridge, M. Donahue, A. Dressler, B. S. Gaudi, T. Greene, O. Guyon, C. Hirata, J. Kalirai, N. J. Kasdin, B. Macintosh, W. Moos, S. Perlmutter, M. Postman, B. Rauscher, J. Rhodes, Y. Wang, D. Weinberg, D. Benford, M. Hudson, W.-S. Jeong, Y. Mellier, W. Traub, T. Yamada, P. Capak, J. Colbert, D. Masters, M. Penny, D. Savransky, D. Stern, N. Zimmerman, R. Barry, L. Bartusek, K. Carpenter, E. Cheng, D. Content, F. Dekens, R. Demers, K. Grady, C. Jackson, G. Kuan, J. Kruk, M. Melton, B. Nemati, B. Parvin, I. Poberezhskiy, C. Peddie, J. Ruffa, J. K. Wallace, A. Whipple, E. Wollack, and F. Zhao. Wide-Field InfrarRed Survey Telescope-Astrophysics Focused Telescope Assets WFIRST-AFTA 2015 Report. *ArXiv e-prints*, March 2015.

[2] A. Carlotti, N. J. Kasdin, and R. J. Vanderbei. Shaped pupil coronagraphy with WFIRST-AFTA. In *Society of Photo-Optical Instrumentation Engineers (SPIE) Conference Series*, volume 8864 of *Society of Photo-Optical Instrumentation Engineers (SPIE) Conference Series*, page 10, September 2013.

[3] A. J. E. Riggs, N. Zimmerman, A. Carlotti, N. J. Kasdin, and R. Vanderbei. Shaped pupil design for future space telescopes. In *Society of Photo-Optical Instrumentation Engineers (SPIE) Conference Series*, volume 9143 of *Society of Photo-Optical Instrumentation Engineers (SPIE) Conference Series*, page 25, August 2014.

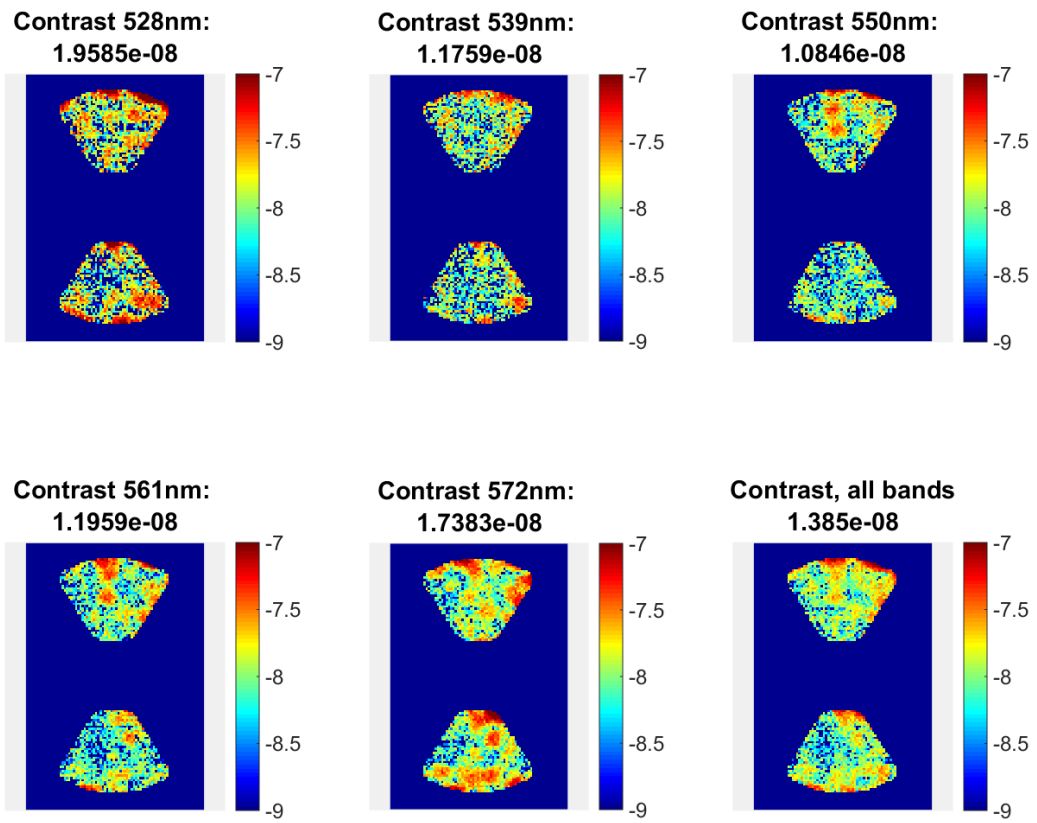

Figure 9. Contrast across 5 2% bands in the Milestone 5 SPLC as of the start of August 2015. Average across the 10% overall band is at lower right.

[4] J. Trauger, D. Moody, and B. Gordon. Complex apodized Lyot coronagraph for exoplanet imaging with partially obscured telescope apertures. In *Society of Photo-Optical Instrumentation Engineers (SPIE) Conference Series*, volume 8864 of *Society of Photo-Optical Instrumentation Engineers (SPIE) Conference Series*, page 12, September 2013.

[5] O. Guyon, P. M. Hinz, E. Cady, R. Belikov, and F. Martinache. High Performance Lyot and PIAA Coronagraphy for Arbitrarily Shaped Telescope Apertures. *The Astrophysical Journal*, 780:171, January 2014.

[6] Neil T. Zimmerman, A J Eldorado Riggs, N. Jeremy Kasdin, Alexis Carlotti, and Robert Vanderbei. Shaped Pupil Lyot Coronagraphs: High-Contrast Solutions for Restricted Focal Planes. *Journal of Astronomical Telescopes, Instruments, and Systems*, submitted, 2015.

[7] Kunjithapatham Balasubramanian, Pierre M. Echternach, Matthew R. Dickie, Richard E. Muller, Victor E. White, Daniel J. Hoppe, Stuart B. Shaklan, Ruslan Belikov, N. Jeremy Kasdin, Robert J. Vanderbei, Daniel Ceperley, and Andrew R. Neureuther. Fabrication and characteristics of free-standing shaped pupil masks for tpf-coronagraph. volume 6265, page 62653N. SPIE, 2006.

[8] Ruslan Belikov, Amir Giveon, Brian Kern, Eric Cady, Michael Carr, Stuart Shaklan, Kunjithapatham Balasubramanian, Victor White, Pierre Echternach, Matt Dickie, John Trauger, Andreas Kuhnert, and N. Jeremy Kasdin. Demonstration of high contrast in 10 percent broadband light with the shaped pupil coronagraph. volume 6693. SPIE, 2007.

[9] I. Poberezhskiy, F. Zhao, X. An, K. Balasubramanian, R. Belikov, E. Cady, R. Demers, R. Diaz, Q. Gong, B. Gordon, R. Goullioud, F. Greer, O. Guyon, M. Hoenk, N. J. Kasdin, B. Kern, J. Krist, A. Kuhnert, M. McElwain, B. Mennesson, D. Moody, R. Muller, B. Nemati, K. Patterson, A. J. Riggs, D. Ryan, B.-J. Seo, S. Shaklan, E. Sidick, F. Shi, N. Siegler, R. Soummer, H. Tang, J. Trauger, J. K. Wallace, X. Wang, V. White, D. Wilson, K. Yee, H. Zhou, and N. Zimmerman. Technology development towards WFIRST-AFTA coronagraph. In *Society of Photo-Optical Instrumentation Engineers (SPIE) Conference Series*, volume 9143 of *Society of Photo-Optical Instrumentation Engineers (SPIE) Conference Series*, page 0, August 2014.

[10] K. Balasubramanian, D. Wilson, V. White, R. Muller, M. Dickie, K. Yee, R. Ruiz, S. Shaklan, E. Cady, B. Kern, R. Belikov, O. Guyon, and N. J. Kasdin. High contrast internal and external coronagraph masks produced by various techniques. In *Society of Photo-Optical Instrumentation Engineers (SPIE) Conference Series*, volume 8864 of *Society of Photo-Optical Instrumentation Engineers (SPIE) Conference Series*, page 1, September 2013.

[11] E. Cady, C. Mejia Prada, X. An, K. Balasubramanian, R. Diaz, N. J. Kasdin, B. Kern, A. Kuhnert, B. Nemati, I. Poberezhskiy, A. J. E. Riggs, R. Zimmer, and N. Zimmerman. Demonstration of high contrast with an obscured aperture with the WFIRST-AFTA shaped pupil coronagraph. *Journal of Astronomical Telescopes, Instruments, and Systems*, submitted, 2015.